

Physics with post-accelerated beams at ISOLDE: nuclear reactions

This content has been downloaded from IOPscience. Please scroll down to see the full text.

2017 J. Phys. G: Nucl. Part. Phys. 44 044013

(<http://iopscience.iop.org/0954-3899/44/4/044013>)

View [the table of contents for this issue](#), or go to the [journal homepage](#) for more

Download details:

IP Address: 188.184.3.52

This content was downloaded on 05/09/2017 at 18:00

Please note that [terms and conditions apply](#).

You may also be interested in:

[Nuclear-structure studies of exotic nuclei with MINIBALL](#)

P A Butler, J Cederkall and P Reiter

[Physics with reaccelerated radioactive beams at TRIUMF-ISAC](#)

G C Ball, L Buchmann, B Davids et al.

[NSCL and FRIB at Michigan State University: Nuclear science at the limits of stability](#)

A Gade and B M Sherrill

[The TRIUMF-ISAC facility: two decades of discovery with rare isotope beams](#)

G C Ball, G Hackman and R Krücken

[Radioactive ion beam physics at the cyclotron research centre Louvain-la-Neuve](#)

Mark Huyse and Riccardo Raabe

[Nuclear structure experiments along the neutron drip line](#)

T Baumann, A Spyrou and M Thoennessen

[Towards detailed knowledge of atomic nuclei -the past, present and future of nuclear structure investigations at GSI](#)

J Gerl, M Grska and H J Wollersheim

[ISOLDE past, present and future](#)

Maria J G Borge and Björn Jonson

Physics with post-accelerated beams at ISOLDE: nuclear reactions

A Di Pietro^{1,4}, K Riisager² and P Van Duppen³

¹ INFN—Laboratori Nazionali del Sud, via Santa Sofia 62, I-95123 Catania, Italy

² Department of Physics and Astronomy, University of Aarhus, DK-8000 Aarhus C, Denmark

³ KU Leuven, Department of Physics and Astronomy, Instituut voor Kern-en Stralingsfysica, B-3001 Leuven, Belgium

E-mail: dipietro@lns.infn.it, kvr@phys.au.dk and Piet.VanDuppen@kuleuven.be

Received 8 November 2016, revised 27 January 2017

Accepted for publication 15 February 2017

Published 10 March 2017



CrossMark

Abstract

Nuclear-reaction studies have until now constituted a minor part of the physics program with post-accelerated beams at ISOLDE, mainly due to the maximum energy of REX-ISOLDE of around 3 MeV/u that limits reaction work to the mass region below $A = 100$. We give an overview of the current experimental status and of the physics results obtained so far. Finally, the improved conditions given by the HIE-ISOLDE upgrade are described.

Keywords: ISOLDE, transfer reactions, elastic scattering, nuclear astrophysics

(Some figures may appear in colour only in the online journal)

1. Introduction

The availability of post-accelerated radioactive ion beams in the 1–20 MeV/u region opens a new window of opportunity to study the atomic nucleus as nuclear reaction studies below and above the Coulomb barrier become possible. These studies should result in physics observables that can be compared to state-of-the-art theory and advance our understanding of the nuclear structure and reaction dynamics. An overview of the status of the field and its current and future radioactive beam facilities is given in the proceedings of a recent symposium [1].

At REX-ISOLDE, reaction studies focus on research questions related to the structure of light nuclei, the influence of halo structures on the reaction dynamics and the evolution of neutron single-particle states around neutron shell and subshell closures. The maximum available energy from the room temperature accelerator (3.3 MeV/u) limited the reaction

⁴ Author to whom any correspondence should be addressed.



studies to elastic and in-elastic scattering, break-up and few-nucleon transfer reactions and also restrained the mass region that could be studied. Some of the lightest nuclei close to or at the neutron dripline, reveal a neutron halo (see e.g. [2, 3]). This intriguing phenomenon, that is due to tunneling of one or two loosely bound neutrons outside the nucleus, has been investigated using several different experimental probes and more details on halos are reported in [4, 5]. With the new beams from REX-ISOLDE further characterization of halos and studies of neutron unbound states, using few-nucleon transfer reactions, became possible.

Recently, it has become clear that halo structures also largely affect the reaction dynamics (see e.g. [6–9]). Due to strong coupling to the continuum of Coulomb and nuclear origin, elastic scattering cross-sections involving halo nuclei show the typical behavior observed in the case of long-range absorption effects. Moreover, as expected, break-up cross-sections are enhanced, owing to the low break-up threshold of halo nuclei. These findings led to the development of complex reaction model calculations e.g. [10, 11] that are being validated with elastic scattering and break-up reactions studies at ISOLDE. In heavier nuclei, the evolution of single-particle states when moving away from the line of stability is a topic of great current interest [12]. Specific components of the nucleon–nucleon interaction, like e.g. the tensor interaction [13] or three-body forces [14, 15] induce shifts in the neutron and proton orbitals when changing proton or neutron number respectively. Consequently, shell gaps, known close to stability, disappear and new ones appear giving rise to phenomena like an ‘island of inversion’ or low-lying 0^+ states based on multi-particle multi-hole excitation across closed shells (see e.g. [16] and references therein). These phenomena were studied around closed neutron shells using one and two neutron transfer reactions.

In this contribution we give a short review of the different reaction experiments performed and the instrumentation used with the REX-ISOLDE beams. The paper is organized in a number of sections that deal with the experimental conditions and the instrumentation (section 2), results obtained in the light nuclei (section 3), studies around closed neutron shells (section 4) and reactions of interest for nuclear astrophysics (section 5). The paper closes with a summary and an outlook focussed on the new opportunities that become available with the HIE-ISOLDE accelerator. More information can be found in [17, 18].

2. Experimental conditions and instrumentation

2.1. Radioactive beam characteristics

We refer to [17] for a general overview of the REX-ISOLDE accelerator. It may be useful to highlight here some of its technical properties relevant for nuclear-reaction studies. A major advantage of the REX-ISOLDE concept is that any one out of the many sufficiently intense radioactive 1^+ beams from ISOLDE may be accepted, charge bred and accelerated with an efficiency typically between 5% and 10%. The price for this universal scheme is a delay in delivery that, in the worst cases (for heavy elements), may be of the same order as the effusion and diffusion time of the radioactive atoms out of the ISOLDE target. Substantial fractions of short-lived isotopes, i.e. with half-lives of the order of 100 ms or less, can therefore decay during the beam preparation phase. In principle this can introduce the daughter nucleus as a beam component, but in practice this has not been a significant problem. For certain, mainly light mass, isotope contamination of stable beams is a more serious problem. Some may arise from the ISOLDE targets and be brought along with the isotope of interest, some are produced from the residual gas in the REX-EBIS charge breeder. The latter can be quite strong for certain isotopes, an example being ^8Li where both ^{12}C and ^{16}O (the two strongest induced beams from the REX-EBIS) will occur on charge state 2^+ , with ^{16}O also present on charge

state 3^+ . One way to decrease such components is to insert stripper foils during acceleration. Other examples are beryllium beams where ^{22}Ne and ^{20}Ne enriched gases are used in REX-TRAP to avoid contaminations, in the case of ^{10}Be and ^{11}Be isotopes, respectively. Some ISOLDE targets deliver, or can be made to deliver, molecular beams. Molecular contaminants will in general not be a problem, since they will be dissociated at latest in REX-EBIS. In some cases one may also select the wanted isotope in a molecular form for injection into the REX-TRAP either in order to suppress a too high isobaric contamination or in order to get higher yields (for elements such as carbon and nitrogen).

The time structure of REX-ISOLDE beams varies from beam time to beam time. The 1.4 GeV proton beam from the PB-Booster is pulsed and distributed in a supercycle to different users at CERN. The minimum time between pulses is 1.2 s and ISOLDE typically gets one third or less of the pulses. The radioactive ions produced in the target will diffuse out before being ionized and transported to the low-energy stage of REX. The typical timescale for this can be as low as 0.1 s, but will vary quite a lot for different elements and different targets. The repetition rate of the low-energy stage of REX depends mainly on the necessary breeding time of the REX-EBIS to achieve the required A/q ratio. This may, for the lightest ions, be just a few ms in which case the rate may be increased to 49 Hz. For many intermediate mass ions a 10 Hz repetition rate is used, but for the heaviest ions this will decrease to a few Hz. The REX-EBIS pulse length can vary from a few tens of microseconds up to an order of magnitude longer. Finally, the accelerated beam has a further microstructure on the 10 ns scale. All these factors taken together give a rather high instantaneous rate compared to the overall average rate.

It is unavoidable that a small fraction of the radioactive beam is deposited inside the scattering chambers and there was initially a worry that this could enhance the background in reaction experiments. For a few long-lived isotopes the remaining radioactivity is a real concern, but more in the low-energy stage than in the experiments. The experience so far is that the deposited activity can be reduced sufficiently to be irrelevant by looking only at events occurring within the EBIS gate, see for an example figure 2 in [19].

2.2. Experimental set-ups

In order to perform reaction studies, dedicated detection systems have been installed at ISOLDE. Since the beam intensities of the most exotic beams are typically small (10^3 – 10^6 pps), relatively thick targets are to be used, and the detection set-ups must be as efficient as possible, e.g. covering a large solid angle. Many of the reaction studies are performed in inverse kinematics; in these cases, the limited beam energy at REX-ISOLDE, up to 3 MeV/u, implies that the largest cross-section in many reaction channels, such as elastic and inelastic scattering or transfer reactions on light targets, correspond to outgoing light reaction products of low energy that are difficult to measure. For these studies the set-ups employed so far have focussed on detection of outgoing charged particles in Si-detector arrays and/or γ -rays in Ge-detector arrays. Other detection set-ups, based on silicon detector telescopes, having flexible geometry that can be adapted to the requirements of the different type of experiments, have been installed at REX-ISOLDE and used for reaction studies with light beams both in inverse and direct kinematics. Detection of beam-like particles in spectrometers or of neutrons have not yet been implemented. In the following we will describe some of the set-ups that have been used for reaction studies with post-accelerated beams at ISOLDE.

2.2.1. The Miniball-array. The Miniball spectrometer has been in operation at REX-ISOLDE for over 10 years, mainly with the aim of studying nuclear structure using transfer or

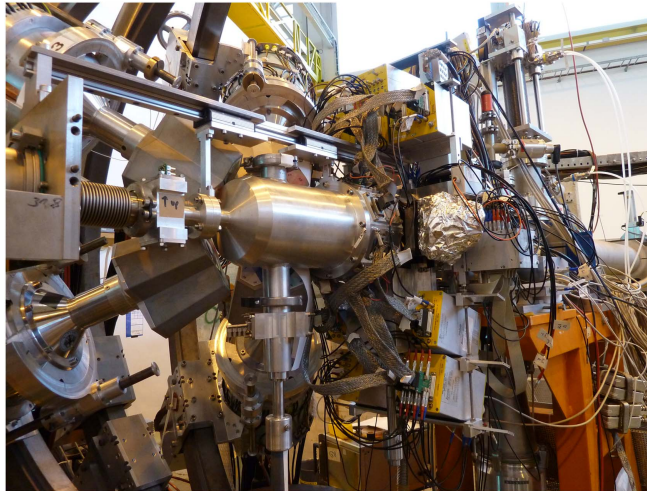


Figure 1. A photo of the T-REX reaction chamber that hosts the Si detector array. Four out of eight capsules of the Miniball germanium array are put in position, the other half was retracted. The ISOLDE post-accelerated beam enters the chamber from the left. On the bottom side of the reaction chamber the targets and beam diagnostics holder can be seen. Reproduced with permission from V. Bildstein.

Coulomb excitation reactions. This high-resolution germanium detector array, consists of 24, six-fold segmented, encapsulated high-purity crystals, specially designed for low multiplicity experiments with low-intensity radioactive ion beams. A complete review can be found in [20]. With radioactive beams, transfer reactions or Coulomb excitation experiments are performed in inverse kinematics, leading to particles emitting the γ -rays of interest being the projectile-like fragments; a large Doppler-shift correction is therefore required. This correction depends upon the opening angle between the scattered ion and the γ -ray, and its precision is determined by the segmentation of the detector system. Each Miniball crystal is 78 mm in height and 70 mm in diameter; it has a quasi-cylindrical shape with a hexagonally shaped front end. The outer electrodes are six-fold segmented providing six segment signals, while the sum energy is obtained from the core electrode.

The combination of electrode segmentation and pulse shape analysis enables the determination of the first interaction point of the γ -ray within a single crystal. For the core signal, in a detector with an approximately cylindrical geometry, an indication of the radius at which the interaction takes place can be obtained from the ‘time-to steepest-slope’. This is a direct measure of the drift time for the corresponding charge carriers, namely, the distance those charge carriers travel to migrate from the interaction point to the electrode. In addition to the radial position information, in segmented detectors the azimuthal information can be obtained using another effect: transient charges, generated by the charge collection process within one segment, induce mirror charges on the adjacent segments. The amplitude of the mirror charges depends upon the distance between the charge carriers and the segment boundary. Hence, by comparing the mirror charge amplitudes in segments on either side of the one in which the interaction took place, it is possible to obtain the azimuthal position. Typical multiplicities in experiments at REX-ISOLDE are low, for this reason Miniball relies on the determination of the position of the main interaction in two dimensions rather than the first interaction in three dimensions as in the AGATA array [21]. In Miniball a spatial

resolution of about 7.5 mm was obtained in laboratory tests of the prototype, leading to a granularity of about 100 pixels. With the detectors placed at 10 cm from the reaction target, the geometrical coverage of the Miniball array corresponds to 60% of 4π with a full-energy peak efficiency that varies from $\approx 25\%$ at 150 keV to $\approx 8\%$ at 1.5 MeV.

The polar angular position of each detector is approximately 45° (for the forward detectors) or 135° (for the backward detectors) with respect to the beam line. In the azimuthal direction, the four clusters at forward and backward angles, are positioned on a circle, separated by 90° . The measured energy resolution (FWHM) with standard ^{152}Eu calibration source goes from 2 keV for 150 keV γ -rays to about 3 keV for 1.5 MeV γ -rays. Details for the in-beam resolutions can be found in [20].

2.2.2. T-REX. Traditionally, transfer reactions have been studied using collisions of light beams (p, d, t, ^3He , α) on heavy targets. To extend the studies of transfer reactions to radioactive beams, as mentioned before, inverse kinematic experiments must be performed. T-REX was designed to measure (d,p) and (t,p) reactions in inverse kinematics at ISOLDE in combination with the Miniball array. To achieve this, the detector design had to satisfy six main requirements: large angular and solid angle coverage, particle identification of the light recoiling particles, angular resolution to reduce kinematical broadening, compact set-up and a low material budget for use inside the Miniball array. A sketch of the T-REX+Miniball set up is shown in figure 1.

T-REX is an array of silicon detector telescopes [23]. The angular range on either side of 90° is covered by two four-sided barrels; the ΔE stages are made of position sensitive silicon strip detectors, $50 \times 50 \text{ mm}^2$, $140 \mu\text{m}$ thick, segmented into 16 resistive strips perpendicular to the beam direction, while the E stages are single pad silicon detectors $1000 \mu\text{m}$ thick. The forward and backward angular ranges are covered by two, four quadrant, CD-PAD telescopes. Annular, double-sided silicon strip detector (DSSTD) [22] were used with 500 and $140 \mu\text{m}$ thickness ΔE , downstream and upstream respectively. Each quadrant has 16 annular junction strips with a 2 mm pitch and 24 sector ohmic strips. The annular and sector strips provide θ and ϕ for the scattered heavy-ion. The forward detectors are protected by a thin foil, which stops the beam particles scattered by the heavy element of a molecular target. When required, also the backward detectors are equipped with protection foils. With the chosen detector thickness, protons above 5–7 MeV, depending upon angle, are identified. For low energy protons, stopping in the ΔE detector, the E detector can be used as a veto to reduce the electron background of β -decay origin; otherwise the low energy proton spectrum would be heavily contaminated. The total solid angle coverage of the T-REX array is about 60% of 4π . The energy resolution of T-REX is limited by kinematical broadening due to the angular resolution of the array, the energy spread in the target thickness and, in the backward direction, the kinematic compression. Owing to these limitations in many cases the Miniball array is used to identify states populated in transfer reactions via their characteristic γ -rays.

2.2.3. Other experimental set-ups. For some of the light beams one will mainly populate particle-unbound states so that there are very few γ -rays of interest decaying from the final state. Furthermore, other types of reaction studies can be performed in order to investigate, not only nuclear structure but also reaction dynamics. For this reason it can be advantageous to have more flexibility in designing the geometry of the Si-detectors and/or their thickness. In such cases different set-ups have been used in other scattering chambers. This was in particular the case for the first generation of transfer reaction experiments that took place before T-REX was constructed but also for studies aimed at investigating how nuclear structure, in particular the halo structure, influences the reaction dynamics. For these

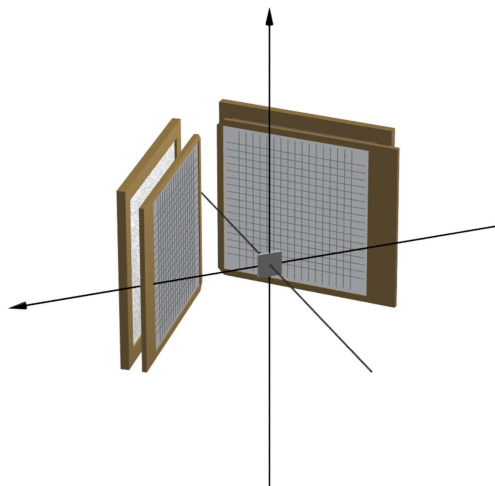


Figure 2. Sketch of the set-up used in 2005 runs used with ^9Li and ^{11}Be beams. The beams react in targets placed at the origin of the coordinate system and charged reaction products are recorded in Si-telescopes placed at each side of the beam, see text for details.

experiments arrays of silicon-detector-telescopes have been used. An example is shown in figure 2: two pairs of detectors are placed at each side of the beam viewing the forward going charged particles. Each pair consists of a DSSSD detector (often $60\ \mu\text{m}$ thick) backed by an unsegmented Si detector about 1 mm thick. In other experiments performed at ISOLDE, up to six of these telescopes surrounding the target have been installed. For the installation of these type of set-ups, a general purpose large scattering chamber was later installed in the ISOLDE hall and used e.g. for the ^{30}Mg elastic scattering experiment mentioned in section 3.2. It consists of a 1 m diameter, 50 cm high and 20 mm thick stainless steel vacuum chamber with eight ports. The lid can be removed for installation of interchangeable set-ups.

3. Reactions with light nuclei

REX-ISOLDE was originally conceived for Coulomb excitation and neutron transfer reactions with nuclei with mass number A less than 52. The very light nuclei were therefore a natural focus for the first round of experiments. This region of the nuclear chart has yielded many surprising results during the last decades [2, 3], most importantly the discovery of the halo structure in neutron dripline nuclei. The halo structure emerges here when the last one or two neutrons are sufficiently loosely bound that they can tunnel far outside the nucleus, see [4, 5] for recent status reports on our knowledge of halos. Elastic resonance scattering on H targets and transfer reaction experiments have been performed at REX-ISOLDE in order to investigate the structure of light nuclei. Besides nuclear structure investigations, experiments performed at ISOLDE have highlighted how the dynamic of reactions, at Coulomb barrier energies, is influenced by the very peculiar structure of the halo.

We shall here review the contributions made at REX-ISOLDE for reactions of light nuclei, including reaction dynamic studies, and divide the discussion according to the type of investigation performed.

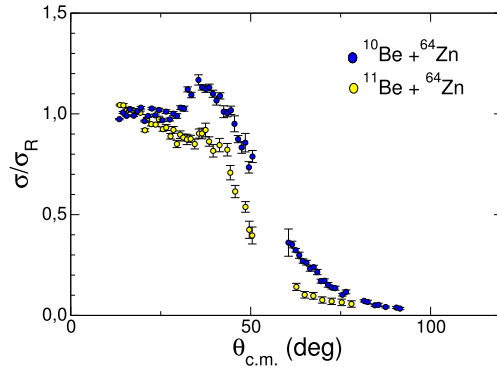


Figure 3. Comparison of $^{10}\text{Be}+^{64}\text{Zn}$ (blue symbols) and $^{11}\text{Be}+^{64}\text{Zn}$ (yellow symbols) scattering angular distribution.

3.1. Investigation of halo structure effects on elastic scattering and break-up

The structure of halo nuclei, with their low break-up threshold and extended matter distribution, can strongly affect the reaction process (for reviews see e.g. [8, 9, 24]). The measurement of elastic scattering is interesting for many reasons; the optical potentials derived from the analysis of elastic scattering angular distributions are required for analyzing other reaction processes like transfer or break-up and its cross-section may strongly depend upon structural properties of the colliding nuclei. Internal degrees of freedom can be excited during the scattering process and coupling effects become relevant. In the case of halo nuclei, coupling to continuum has additional influences; they have large $B(E1)$ strength just above the threshold [25] so they are easily polarizable. The excitation of this low-lying strength via the long range Coulomb field will induce the break-up of the halo, moreover, coupling to this strength affects also the other reaction process. At REX-ISOLDE it was available the first post-accelerated ^{11}Be , In-halo beam, for reaction studies around the Coulomb barrier. Using this beam, the $^{11}\text{Be}+^{64}\text{Zn}$ was measured and, as a comparison, the reaction $^{10}\text{Be}+^{64}\text{Zn}$ was also measured at ISOLDE [26, 27]. The mean ^{11}Be beam intensity was $\sim 7 \times 10^3$ pps while in the case of ^{10}Be was almost three orders of magnitude more (5×10^6 pps).

A stable beam contamination in the Beryllium beams was due to the Boron material of the REX-EBIS cathode. In order to strongly reduce this contaminant, a stripper foil ($25 \mu\text{g cm}^{-2} \text{ }^{12}\text{C}$) was placed just before the last analyzing magnet placed upstream the scattering chamber. Fully stripped Beryllium and Boron ions were emerging from the stripper foil and they were separated in A/q by the dipole field. In a test experiment made before the measurement, the residual Boron contamination was estimated to be $\leq 0.3\%$.

The beam energies upon entering the target were 2.71 MeV/u for ^{11}Be and 2.91 MeV/u for ^{10}Be . For this experiment an array of 6 Si-detector telescopes, surrounding the target, were used. Due to statistics only data gathered in the detectors placed in the forward hemisphere were analyzed.

The experimental data showed a clear change in the reaction mechanism, namely a suppression of the Coulomb-nuclear interference peak, similar to what observed in scattering of very deformed projectiles or targets [28], along with an overall suppression of the elastic cross-section. In figure 3 a comparison of $^{10}\text{Be}+^{64}\text{Zn}$ and $^{11}\text{Be}+^{64}\text{Zn}$ scattering angular distribution is shown. Theoretical analysis using CDCC method, indicates that the suppression of the interference peak is caused by both Coulomb and nuclear couplings to break-up

channels where, the nuclear coupling gives mostly absorptive effects (target excitation, n-transfer or ^{10}Be absorption) and the Coulomb coupling contribute to elastic-breakup of ^{11}Be where none of the fragments is absorbed or excited. The suppression of the Coulomb-nuclear interference peak has been studied also in [29] within the optical model; the combined effect of Coulomb and nuclear interactions between the elastic channel and the high-density breakup states leads to a phase-change of the Coulomb-nuclear interference term which becomes destructive. Both, the Coulomb-nuclear interference and the long-range absorption are interconnected, and caused by the coupling to the continuum states.

^{11}Be has a deformed core, it has been found that core excited components in the g.s. wave function of ^{11}Be , as well as core-dynamic-excitations, influence the dynamics of the break-up, although, at low energy the dynamic effect is found to be small [11, 30]. The ^{10}Be angular distribution of the $^{11}\text{Be} + ^{64}\text{Zn}$ reaction is not well reproduced by the CDCC calculations. CDCC calculations include only the elastic break-up contribution to the cross-section; however, the inclusive measurement of ^{10}Be fragments does not allow the exclusion of other processes, like neutron-transfer, inelastic excitation of the target etc, (non-elastic break-up) to contribute [31]. The non-elastic break-up was found to be the relevant mechanism in the break-up of weakly-bound stable nuclei in the whole angular range [31]. In the case of halo nuclei, the dominant contribution is still elastic break-up, owing to the large low-lying B(E1) strength, however, at larger angles non-elastic processes could become important.

3.2. Elastic resonance scattering

Elastic resonance scattering is an attractive experimental method for investigating the nuclear structure of light nuclei for beams of weak intensity. In this method the beam is stopped (or slowed down by an appreciable amount) inside a target. Reactions that take place during the slowing down and that lead to a light product being emitted in forward direction can then be efficiently measured. This general technique is used in particular for elastic scattering of the beam on hydrogen or helium in the target and enables measurement of the excitation function over an extended energy region in a single run. The technique is often combined with the use of an active target [32], but can also be employed with solid ‘standard’ targets that are easier to incorporate in existing set-ups. Elastic proton-resonance scattering was tried at an early stage of REX with a ^9Li beam [33] and has recently been applied to ^{30}Mg [34]. There are several existing proposals to continue the use of the technique.

In the case of the ^{30}Mg experiment, the isotope was charge bred to 7^+ and accelerated to 2.92 MeV/u, the beam intensity was 1×10^5 pps. The reaction target was a 5.6 mg cm^{-2} thick polyethylene foil, the carbon background was estimated by use of a 10.9 mg cm^{-2} carbon target. The incoming beam was collimated by a 5 mm diameter aperture 1.5 m upstream of the target and a 10 mm diameter aperture just upstream of the target, thereby restricting incident angle to less than 0.28° . At 115 mm downstream a 32×32 strip $58 \times 58 \text{ mm}^2$ $310 \mu\text{m}$ thick DSSSD detector with a $1000 \mu\text{m}$ thick backing Si-PAD detected the outgoing elastically scattered protons. Analysis of the recorded excitation function showed the isobaric analogue resonances in ^{31}Al corresponding to the three lowest states in ^{31}Mg . The energy position, proton width and total width could be extracted for the three states from which spectroscopic factors were deduced. These indicated a drastic change in structure between ^{30}Mg and ^{31}Mg , consistent with other evidence pointing to border of the island of inversion being placed here.

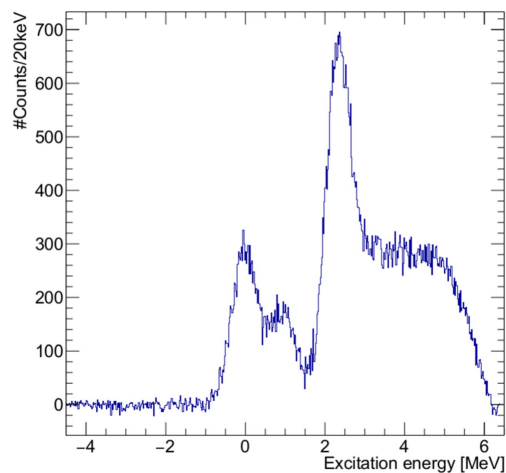


Figure 4. The excitation energy spectrum extracted at 2.8 MeV/u from the ${}^9\text{Li}(d,t){}^8\text{Li}^*$ reaction. The three peaks are due to population of the 2^+ ground state and the two lowest excited states (1^+ and 3^+). The plateau at higher energies starts at the threshold for neutron emission.

3.3. Transfer reaction studies

When intensities of around 10^5 pps are available it is possible to look also for transfer reactions. The largest cross sections typically occur for reactions on a hydrogen target (p or d) and the corresponding theoretical treatments are also rather advanced, so the transfer reaction studies at REX described in the following are of this type.

The first transfer reaction experiments started with tests as soon as REX-ISOLDE came on-line in 2001 and an initial experiment employing a ${}^9\text{Li}$ beam at 2.36 MeV/u took place in the summer of 2002. For this, as well as a second run campaign with ${}^9\text{Li}$ and ${}^{11}\text{Be}$ beams in 2005 (with energies now raised to about 3 MeV/u), the simplified set-ups mentioned above were used, see figure 2. Later experiments with ${}^8\text{Li}$ and ${}^{11}\text{Be}$ beams have made use of more complex set-ups, including T-REX combined with Miniball that was employed for a 2010 run with ${}^{11}\text{Be}$. For this case, detection of final state γ -rays was essential in order to separate in particular the four excited levels in ${}^{10}\text{Be}$ that lie within about 300 keV. For the experiments with beams of ${}^{8,9}\text{Li}$ the final states were sufficiently well separated to be resolved with detection of charged particles only. See figure 4 for an illustration of the resolution obtained. Apart from the physics results an important additional outcome of this series of experiments has been a characterization of the properties of the REX beams, culminating in the detailed investigation of the beam shape based on coincidence data with a well known final two body state [35].

The first ${}^9\text{Li}$ experiment [19] used the 2^+ charge state to avoid background from ${}^{12}\text{C}$ and reached an intensity of about 5×10^4 ions/s with a 20% contamination of the stable ${}^{18}\text{O}$. The beam out of REX-EBIS had a repetition rate of 49 Hz and a pulse length of about 35 μs . Several two-body final state reaction channels were populated and clearly separated allowing angle and energy differential cross sections to be extracted. The excited states seen in the ${}^8\text{Li} + t$ channel were compared to DWBA calculations and the extracted spectroscopic factors [36] found to be larger than those from both the Cohen-Kurath shell model and Quantum Monte Carlo calculations. The compound reaction contribution was evaluated to be small, pointing to the need to use more sophisticated reaction models in these close-to-unbound

systems. The coupled-channels Born approximation method was therefore used for interpreting the $^{10}\text{Li}+p$ data [37]. The angular distributions are here not very distinctive, but the energy spectrum shows a virtual s-state with scattering length of the order of 13–24 fm as well as a p-wave resonance at about 0.4 MeV excitation energy. A total of four states, 1^- , 2^- , 1^+ and 2^+ , are expected when coupling the neutron spin to the spin of ^9Li , but not all may be populated here due to the low beam energy. The structure of the unbound ^{10}Li is still being investigated since it is needed for understanding the composition of the two-neutron halo nucleus ^{11}Li .

The discrepancies found in the modeling of the $^9\text{Li}(d,t)$ experiment triggered a follow-up $^8\text{Li}+d$ experiment [38]. A charge state 2^+ beam that had average intensity 1.6×10^6 pps and a considerable stable beam background could be accelerated to 3.15 MeV/u where a stripper foil before the last dipole cut down the stable beam component significantly. A careful theoretical analysis showed that higher-order effects must be taken into account, in particular for the inelastic channel and the (d,t) channel. However, coupled-channels and coupled-reaction-channels calculations were quite successful in describing the data and could now reproduce the magnitude of the transition between the ground states of ^8Li and ^9Li .

The $^{11}\text{Be}+d$ experiment with T-REX mentioned above used a charge state 4^+ beam accelerated to 2.8 MeV/u and reached a beam intensity up to 10^7 pps. With the γ -ray identification the final bound states reached in the (d,p) channel to ^{12}Be [39] as well as in the (d,t) channel to ^{10}Be [40] could be clearly separated. The data were sufficiently complete to rule out the presence of a bound 0^- state in ^{12}Be . A special feature of this nucleus is a low-lying excited 0^+ state, the exact configuration of this state as well as the ground state is still uncertain. A DWBA analysis has problems in reproducing the angular distributions, but indicated a larger spectroscopic factor to the excited 0^+ state than to the ground state, contrary to what several theoretical calculations obtain. The physics results from the $^{11}\text{Be}(d,t)^{10}\text{Be}$ reaction are given in another contribution to this laboratory portrait [40].

4. Few-nucleon transfer reaction studies around closed neutron shells

One and two neutron transfer reaction studies using neutron-rich REX-ISOLDE beams were performed to study the neutron shell closures at $N = 20, 28, 40$ and 50 . Using two-neutron transfer, low-lying 0^+ states were identified and characterized, while one-neutron transfer allowed the study of single-particle states. Studying the evolution of these states and strengths in exotic nuclei sheds light on the influence of e.g. the tensor interaction [13] or three-body forces [14, 15]. These studies are relevant to understand the underlying mechanism of altering shell-gaps far from stability and to identify specific orbitals that enhance collectivity [41, 42]. On the other hand studying low-lying 0^+ states gives information on their neutron two-particle—two-hole character, on phenomena like shape coexistence and the inversion of normal and so-called intruder configurations in semi-magic nuclei [43].

4.1. Two-neutron transfer reactions

Two-nucleon transfer reactions are an excellent tool to probe two-nucleon correlations and configurations in nuclear states. As such they are ideally suited to identify low-lying excited 0^+ states in even–even nuclei and to study their nature. Especially, two-neutron transfer reactions have been intensively used for studies on stable targets using proton or ^3H beams and high-resolution spectrometers (see e.g. [44, 45]). With the availability of energetic radioactive ion beams at ISOLDE and the use of inverse kinematics it became possible to extend the use of this probe further from stability.

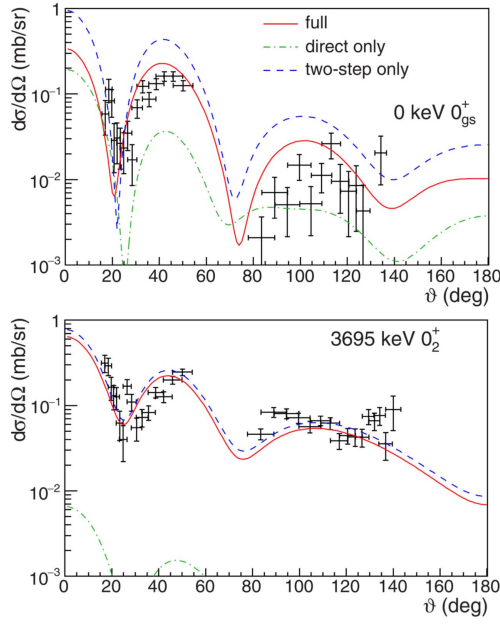


Figure 5. Calculated differential cross section for the two-neutron transfer to the ground state (top), and the first excited 0^+ state (bottom) in comparison with experimental data. The DWBA calculation using direct one-step (green dashed line), two-step (blue dashed line) and both (red solid line) are shown using one- and two-nucleon amplitudes from the SDPF-U effective interaction. Figure adapted with permission from [46]. Copyrighted by the American Physical Society.

Using the REX-ISOLDE beams, low-lying 0^+ states in semi-magic closed neutron shell nuclei at $N = 20$ ($^{30}\text{Mg}(t,p)^{32}\text{Mg}$ [16]), $N = 28$ ($^{44}\text{Ar}(t,p)^{46}\text{Ar}$ [46]) and $N = 40$ ($^{66}\text{Ni}(t,p)^{68}\text{Ni}$ [47]) were investigated to probe the neutron two-particle-two-hole strength. Note that in contrast to the two former reactions, the latter involved a closed proton-shell nucleus ($Z = 28$). Data were also collected for the $^{72}\text{Zn}(t,p)^{74}\text{Zn}$ reaction but have not yet been fully analyzed and interpreted. All experiments used a similar experimental set-up (see section 2). The radioactive beam was sent onto a thin strip of $500 \mu\text{g cm}^{-2}$ thick metallic Ti foil loaded with an atomic ratio $^3\text{H}/\text{Ti}$ of 1.5 corresponding to a target thickness of about $40 \mu\text{g cm}^{-2} \text{ } ^3\text{H}$. The protons were detected with the T-REX silicon array while gamma-rays were recorded in the Miniball germanium detector array.

Figure 5 shows the angular distribution of the differential cross section obtained in the $^{44}\text{Ar}(t,p)^{46}\text{Ar}$ reaction [46]. Feeding of the ground state, first excited 2^+ and 0^+ states were observed. The data were obtained with a beam intensity of 2×10^5 pps at an energy of 2.16 MeV/u. The low beam energy was chosen to avoid fusion reactions with the target carrier material. Gamma decay observed in the Miniball array was used to identify feeding of the different excited states. Angular distributions allowed to determine the angular momentum transfer and thus the spin and parity of the populated states. These differential cross section distributions were also compared with one-step (direct), two-step (sequential) and full (direct + sequential interference) DWBA calculations using general optical potential parameters and one and two neutron amplitudes from different shell-model calculations (see [46] for more details).

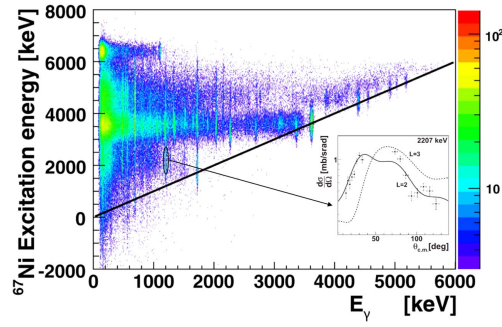


Figure 6. A two-dimensional representation of the Doppler corrected energy of γ rays with respect to the original excitation energy of ^{67}Ni , deduced from proton spectra and kinematics. The color code represents the particle-gamma coincidence intensity. Excited states populated in ^{67}Ni that have a γ -decay branch to the ground state are situated on the diagonal solid black line. The strongest ground state transition at 3621 keV is clearly visible. The inset shows the experimental angular distributions for the $\frac{5}{2}^+$ state at 2207 keV represented by the 1201 keV γ transition to the $\frac{9}{2}^-$ isomer at 1007 keV and an energy window around the 2.2 MeV excitation energy. Fits with $\Delta = 2$ and 3 are shown. Figure adapted with permission from Ref. [49]. Copyrighted by the American Physical Society.

All three investigations showed feeding of a low-lying 0^+ state. In the case of ^{32}Mg and ^{46}Ar these states were newly identified. The population of these excited 0^+ states with respect to the ground-state feeding at low c.m. angles differed substantially for the cases studied: it was about equal in the case of the $^{30}\text{Mg}(t,p)$ and $^{44}\text{Ar}(t,p)$ reaction, while it represented only 4% in case of the $^{66}\text{Ni}(t,p)$. This could be explained by the specific neutron orbitals involved and by cancellation or reinforcing effects of the feeding of specific single-particle orbitals. The agreement between the experimental cross sections and the results from the DWBA calculations, confirms the underlying neutron two-particle two-hole across the closed neutron shell character of the ground state in ^{32}Mg and the excited 0_2^+ states in ^{46}Ar and ^{68}Ni . Population of the first excited 2^+ state was only observed in case of ^{46}Ar and of ^{68}Ni with an approximate intensity relative to the ground-state feeding of 50% and 30% respectively. Moreover, tailored DWBA calculations reproduce the 2^+ feeding in ^{48}Ar but calculate differential cross sections that are over an order of magnitude lower compared to experiment in ^{68}Ni . The latter might be due to the limited model space used for the neutron states or the need for a coupled-reaction-channel calculation taking into account excitations in ^{66}Ni . This issue deserves further investigation.

4.2. Single-particle structures around ^{68}Ni and ^{78}Ni

One-neutron transfer reaction studies have been performed at ISOLDE using the T-REX and Miniball set-up but were, due to the beam energy constraints, limited to light mass nuclei (see section 3) or nuclei around $A = 70$. More specifically, the $^{66}\text{Ni}(d,p)^{67}\text{Ni}$ ($Q_{\text{value}} = 3.580$ MeV), $^{78}\text{Zn}(d,p)^{79}\text{Zn}$ ($Q_{\text{value}} = 1.796$ MeV) reactions were studied to probe the neutron single-particle strength around $N = 40$ and 50 respectively. The relevant neutron orbitals are the $p_{3/2}$, $f_{5/2}$, $p_{1/2}$ below $N = 40$, the $g_{9/2}$ below $N = 50$ and the $d_{5/2}$ and $s_{1/2}$ orbitals above $N = 50$. Especially the positive parity neutron states are assumed responsible for the onset of collectivity in the region of the nuclear chart below ^{68}Ni . It has recently been suggested that the latter is a good candidate for a new island of inversion [59, 60]. The effect

of the quadrupole coherence generated by this quasi-SU(3) sequence ($\Delta j = 2$), containing the $g_{9/2}$ $d_{5/2} s_{1/2}$ orbitals, depends on their relative energy separation and thus on the $N = 50$ gap size. The experiments were performed at a beam energies of 2.95 MeV/u ($^{66}\text{Ni}(d,p)^{67}\text{Ni}$) and 2.83 MeV/u ($^{78}\text{Zn}(d,p)^{79}\text{Zn}$) while the beam intensity was 4.1×10^6 and 7.8×10^5 pps respectively. A thin (about $100 \mu\text{g cm}^{-2}$) deuterated polyethylene target was positioned at the center of the T-REX set-up. Reaction protons were detected in the silicon array while γ -rays in the Miniball array [48–50].

In case of the $^{66}\text{Ni}(d,p)^{67}\text{Ni}$ study, high statistics in particle- γ and γ - γ coincidences was obtained and allowed to construct level schemes and decay characteristics, population cross section and, for the strongest transitions, angular distributions (figure 6). From this information the transferred angular momentum could be deduced restraining the spin/parity values of the resulting states. Because of the presence of the $13 \mu\text{s } \frac{9^-}{2}$ isomer in ^{67}Ni a delayed-coincidence set-up was built. Gamma-rays emitted from this isomer were detected in the beam dump situated 2 m away from the reaction chamber. Using a delayed-coincidence condition, direct and indirect through gamma cascades feeding of the isomer could be determined. From a DWBA calculation, using global optical model potentials, relative spectroscopic factors compared to the $g_{9/2}$ state at 1007 keV were deduced. From a comparison with large-scale shell model calculations it could be shown that the position and relative spectroscopic factor of the $p_{3/2}$, $f_{5/2}$, $p_{1/2}$ relative to the $g_{9/2}$ state were in fair agreement. The relative spectroscopic factors of the $d_{5/2}$ strength show that half of the $\nu d_{5/2}$ single-particle strength is split in nearly equal parts over two $\frac{5^+}{2}$ states indicating substantial mixing of the $d_{5/2}$ configuration with collective core coupled modes. Moreover, the $d_{5/2}$ strength was located at lower energy.

In the $^{78}\text{Zn}(d,p)$ study, population of two distinct level sequences in ^{79}Zn ($N = 49$) were observed and a $\frac{1^+}{2}$ isomer at 1.10 MeV excitation energy was identified. One level sequence decayed to the $\frac{9^+}{2}$ ground state while the second one decayed towards the isomer. Comparison with shell-model calculations indicate involvement of neutron excitation across the $N = 50$ shell closure in the low-lying states [50]. The existence of the $\frac{1^+}{2}$ isomer has been confirmed in recent experiments, and its spin and parity [61], as well as the excitation energy, have been firmly fixed [62] in agreement with [50].

5. Astrophysics

Only a few experiments have been proposed and/or performed at ISOLDE with the aim of studying reactions of astrophysical interest. In fact, the REX-ISOLDE energy range of ~ 1.2 – 3 MeV/u and limited high intensity RIBs has restricted the possibilities for direct and indirect Nuclear Astrophysics measurements.

The $^{14}\text{O}(\alpha,p)^{17}\text{F}$ reaction has implications for the energy generation in explosive burnings in novae and x-ray bursters. Its reaction rate was thought to be dominated by the capture onto the $^{18}\text{Ne } 1^-$ state at 6.15 MeV, which proton decays. Beside the ground state branch, it is suggested [51] that the inelastic branch, leading to ^{17}F excited to its $\frac{1^+}{2}$ at 0.495 keV first excited state, gives a comparable rate to the $^{14}\text{O}(\alpha,p)^{17}\text{F}$ cross-section. In order to study the inelastic component of the $^{14}\text{O}(\alpha,p)^{17}\text{F}$, the reaction $^{17}\text{F}(p,p')$ was studied at REX-ISOLDE [52]. A ^{17}F beam at 44.2 MeV was stopped inside a $\sim 40 \mu\text{m}$ CH_2 target. The recoiling protons were detected into a CD detector telescope of thickness $35 \mu\text{m}$ (ΔE detector) and 0.5 mm (E detector). Protons in coincidence with 0.495 γ -rays detected in Miniball array were measured. The result of this study was that the inelastic proton branch, $^{14}\text{O}(\alpha,p')^{17}\text{F}_{\frac{1^+}{2}}$ has a

comparable influence on the $^{14}\text{O}(\alpha,p)^{17}\text{F}$ than to the ground-state branch, but somewhat smaller than previously suggested in [51].

One of the reactions responsible for the ^{44}Ti destruction in supernovae is the $^{44}\text{Ti}(\alpha,p)^{47}\text{V}$, thus the final amount of ^{44}Ti in supernovae depends upon the reaction rate of this reaction. The $^{44}\text{Ti}(\alpha,p)^{47}\text{V}$ was measured at REX-ISOLDE. For this experiment the ^{44}Ti beam was produced in batch-mode rather than with the usual ISOL technique. With this beam production technique, no isotopic beam contaminations were observed. A 50MBq ^{44}Ti ($T_{1/2} = 59.2$ y) sample dissolved in HF and then evaporated in molybdenum was prepared at Paul Scherrer Institute (PSI) [53] and then shipped at CERN. Details of the radioactive beam production can be found in [54]. The ^{44}Ti beam intensity on target ranged from 5×10^5 to 2×10^6 pps. The target consisted in a gas-cell with Al windows, containing 67 mbar ^4He gas; the thickness of the exit window was chosen to stop the beam-like particles. The c.m. energy of the beam on target was 4.15 MeV which was within the relevant Gamow window. Protons were detected by an MSL type S2 annular DSSSD ΔE -E particle telescope with a ΔE thickness of 65 μm and an E thickness of 1000 μm . The detailed data analysis performed showed no evidence of protons coming from the $^{44}\text{Ti}(\alpha,p)^{47}\text{V}$ reaction, thus providing an upper limit for this cross-section of 40 μbarn [54].

There have been three more proposals on reaction studies of astrophysical interest: $d(^7\text{Be}, p)$ [55] reaction related to the cosmological ^7Li problem; the study of nuclear structure of ^{18}N [56] related to the heavy element production in r-processes; the reaction $^{59}\text{Cu}(p,\alpha)$ [57] important for the heavy element synthesis in the νp -process [58].

6. Conclusion and outlook

The reaction work carried out until now at REX-ISOLDE has demonstrated the large physics potential in such studies, but also illustrated the clear need for improvements in experimental conditions. Several shortcomings are already being remedied in the HIE-ISOLDE project [18, 63] as described briefly in the following.

The most important improvement is the increase of beam energy. It has already been raised from 3 to 5.5 MeV/u and will increase further to 10 MeV/u in 2018. These maximum energies are for charge states giving $A/q = 4.5$, for higher charge states even larger energies can be reached. The added superconducting acceleration cavities are sufficiently flexible to allow the beam energy to be tuned from the current range up to the maximum. The energy increase will take all accelerated beams at ISOLDE above the Coulomb barrier and thereby enable reaction studies even for the heaviest produced isotopes. The increase will also make transfer reactions more sensitive to the angular momentum transferred and simplify the theoretical interpretation of the results. One can extend the investigation to reactions with an unfavorable Q_{value} including other two nucleon-transfer reactions, two-proton and deuteron transfer and possibly alpha particle transfer like e.g. $^{64}\text{Fe}(^6\text{Li}, ^2\text{H})^{68}\text{Ni}$. This will open up a new region of the nuclear chart to study nucleon–nucleon correlations as well to investigate the underlying nucleon-structure of the populated states. An important ingredient to fully exploit this sensitive probe is the improvement and further development of reaction theory. For nuclear astrophysics the higher beam energies offers opportunities for indirect (e.g. transfer reactions), and direct (e.g. time-reversed (α,p)) measurements.

The HIE-ISOLDE project also encompasses intensity upgrades and beam quality improvements. This will lead to data of higher quality and statistics than currently obtainable, but will also allow new types of studies to be undertaken. Two examples are more exclusive measurements and sub-barrier fusion studies.

The benefits of the accelerator upgrades are further enhanced by the introduction of new experimental equipment. New set-ups for reaction experiments include the ISOLDE Superconducting Solenoid (ISS) that is currently being prepared for installation in the experimental hall. It is based on the successful HELIOS spectrometer at Argonne that, by effectively measuring particle tracks in a strong magnetic field, increases the achievable resolution considerably. When efficiency rather than resolution is the main concern, active targets are a very attractive possibility, and proposals to employ the future ACTAR device at ISOLDE have already been submitted. To further enhance the existing Miniball set-up the plan is to reuse part of the TRI μ P spectrometer from KVI as a zero-degree High-ISOLDE Fragment Identifier spectrometer to detect also heavy beam-like fragments with high efficiency and resolution. All this gives new opportunities for reaction experiments.

Looking further into the future, installing a storage ring behind HIE-ISOLDE would give very interesting new physics possibilities. The science case and a technical design study [64] for moving the TSR to ISOLDE has been prepared, but a positive final decision on this option is still waiting. The physics case is sufficiently attractive to warrant further work in this direction.

In conclusion, the first generation of reaction experiments at ISOLDE have demonstrated the huge potential in reaction studies with radioactive beams at and above the Coulomb barrier. With the addition of the current accelerator and instrument upgrades at ISOLDE, a very interesting physics program is ensured for the next decade or more.

Acknowledgments

The authors would like to thank JH Jensen for assistance with figures and T Davinson for useful discussions. KR would like to acknowledge the Danish Natural Science Research Council for support. PVD acknowledges the support from Research Foundation—Flanders and the IAP network program P7/12 (Belgian Science Policy office).

References

- [1] Fahlander C and Jonson B 2013 Nobel symposium 152: physics with radioactive beams *Phys. Scr. T* **152** 010301
- [2] Jonson B 2004 *Phys. Rep.* **389** 1–59
- [3] Chulkov L V, Jonson B and Zhukov M V 2015 *Eur. Phys. J. A* **51** 97
- [4] Tanihata I, Savajols H and Kanungo R 2013 *Prog. Part. Nucl. Phys.* **68** 215–313
- [5] Riisager K 2013 *Phys. Scr. T* **152** 014001
- [6] Keeley N, Alamanos N, Kemper K W and Rusek K 2009 *Prog. Part. Nucl. Phys.* **63** 396
- [7] Lapoux V and Alamanos N 2015 *Eur. Phys. J. A* **51** 19
- [8] Canto L F, Gomes P R S, Donangelo R, Lubian J and Hussein M S 2015 *Phys. Rep.* **596** 1
- [9] Kolata J J, Guimaraes V and Aguilera E F 2016 *Eur. Phys. J. A* **52** 123
- [10] Rodríguez-Gallardo *et al* 2008 *Phys. Rev. C* **77** 064609
- [11] de Diego R, Arias J M, Lay J A and Moro A M 2014 *Phys. Rev. C* **89** 064609
- [12] Sorlin O and Porquet M G 2008 *Prog. Part. Nucl. Phys.* **61** 602
- [13] Otsuka T *et al* 2010 *Phys. Rev. Lett.* **104** 012501
- [14] Zuker A P *et al* 2003 *Phys. Rev. Lett.* **90** 042502
- [15] Hagen G *et al* 2012 *Phys. Rev. Lett.* **109** 032502
- [16] Wimmer K *et al* 2010 *Phys. Rev. Lett.* **105** 252501
- [17] Van Duppen P and Riisager K 2011 *J. Phys. G: Nucl. Part. Phys.* **38** 024005
- [18] Blaum K, Borge M J B, Jonson B and Van Duppen P 2015 *Adv. Ser. Dir. High Energy Phys.* **23** 415
- [19] Jeppesen H B *et al* 2005 *Nucl. Phys. A* **748** 374–92

- [20] Warr N *et al* 2013 *Eur. Phys. J* **49** 40
- [21] Simpson J *et al* 2015 *Eur. Phys. J. A* **606** 012017
- [22] Ostrowski A *et al* 2002 *Nucl. Instrum. Methods A* **480** 448
- [23] Bildstein V *et al* 2012 *Eur. Phys. J. A* **48** 85
- [24] Kolata J J, Guimarães V and Aguilera E F 2016 *Eur. Phys. J. A* **52** 123
- [25] Aumann T and Nakamura T 2013 *Phys. Scr. T* **152** 014012
- [26] Di Pietro A *et al* 2010 *Phys. Rev. Lett.* **105** 022701
- [27] Di Pietro A *et al* 2012 *Phys. Rev. C* **85** 054607
- [28] Love W G *et al* 1977 *Nucl. Phys. A* **291** 183
- [29] Diaz-Torres A and Moro A M 2014 *Phys. Lett. B* **733** 89
- [30] Moro A M and Lay J A 2012 *Phys. Rev. Lett.* **109** 232502
- [31] Lei J and Moro A M 2015 *Phys. Rev. C* **92** 044616
- [32] Beceiro-Novo S, Ahn T, Bazin D and Mittag W 2015 *Prog. Part. Nucl. Phys.* **84** 124–65
- [33] Jeppesen H B 2004 *PhD Thesis* Aarhus University unpublished
- [34] Imai N *et al* 2014 *Phys. Rev. C* **90** 011302
- [35] Johansen J G *et al* 2013 *Nucl. Instrum. Methods A* **714** 176–87
- [36] Jeppesen H B *et al* 2006 *Phys. Lett. B* **635** 17–22
- [37] Jeppesen H B *et al* 2006 *Phys. Lett. B* **642** 449–54
- [38] Tengborn E *et al* 2011 *Phys. Rev. C* **84** 064616
- [39] Johansen J G *et al* 2013 *Phys. Rev. C* **88** 044619
- [40] Johansen J G *et al* 2016 *J. Phys. G: Nucl. Part. Phys.* accepted
- [41] Zuker A P *et al* 1995 *Phys. Rev. C* **52** R1741
- [42] Lenzi S M *et al* 2010 *Phys. Rev. C* **82** 054301
- [43] Wood J L *et al* 2016 *J. Phys. G: Nucl. Part. Phys.* **43** 020402
- [44] Meyer D A *et al* 2006 *Phys. Lett. B* **638** 44–9
- [45] Leach K G *et al* 2013 *Phys. Rev. C* **88** 031306(R)
- [46] Nowak K *et al* 2016 *Phys. Rev. C* **93** 044335
- [47] Elseviers J *et al* 2017 in preparation
- [48] Diriken J *et al* 2014 *Phys. Lett. B* **736** 533–8
- [49] Diriken J *et al* 2015 *Phys. Rev. C* **91** 054321
- [50] Orlandi R *et al* 2015 *Phys. Lett. B* **740** 298–302
- [51] Blackmon J C *et al* 2003 *Nucl. Phys. A* **718** 127–30
- [52] He J J *et al* 2009 *Phys. Rev. C* **80** 042801
- [53] Dressler R *et al* 2012 *J. Phys. G: Nucl. Part. Phys.* **39** 105201
- [54] Margerin V *et al* 2014 *Phys. Lett. B* **731** 358–61
- [55] Gupta D 2012 *IOLSDE Proposal* IS554
- [56] Matta A 2013 *ISOLDE Proposal* IS591
- [57] Lederer C 2015 *ISOLDE Proposal* IS607
- [58] Fröhlich C *et al* 2006 *Phys. Rev. Lett.* **96** 142502
- [59] Gade A *et al* 2010 *Phys. Rev. C* **81** 051304
- [60] Lenzi S *et al* 2010 *Phys. Rev. C* **82** 054301
- [61] Yang X F *et al* 2016 *Phys. Rev. Lett.* **116** 182502
- [62] Matea I *et al* 2016 private communication
- [63] Borge M J G and Riisager K 2016 *Eur. Phys. J A* **52** 334
- [64] Grieser M *et al* 2012 *Eur. Phys. J. Spec. Top.* **207** 1–117